

LUDWIG-MAXIMILIANS-UNIVERSITÄT MÜNCHEN
FACULTY OF PHYSICS

Evaluation of the South Asian Monsoon in the ECHAM/MESSy Atmospheric Chemistry model

Alexander Haluszczynski



June 2014

LUDWIG-MAXIMILIANS-UNIVERSITÄT MÜNCHEN

FAKULTÄT FÜR PHYSIK

Evaluation des südostasiatischen Monsuns im ECHAM/MESSy Atmospheric Chemistry Modell

Alexander Haluszczynski



Juni 2014

LUDWIG-MAXIMILIANS-UNIVERSITÄT MÜNCHEN
FACULTY OF PHYSICS

Evaluation of the South Asian Monsoon in the ECHAM/MESSy Atmospheric Chemistry model

Alexander Haluszczynski

BACHELOR THESIS



Supervisor: Priv.-Doz. Dr. habil. Veronika Eyring (DLR)

Deutsches Zentrum für Luft- und Raumfahrt (DLR)
Institut für Physik der Atmosphäre

June 2014

Abstract

The South Asian Monsoon has been evaluated in the ECHAM/MESSy Atmospheric Chemistry (EMAC) model in comparison to observations and models participating in the 5th Phase of the Coupled Model Intercomparison Project (CMIP5). Existing diagnostics of the Earth System Model Evaluation Tool (ESMValTool) have been applied to historical CMIP5 simulations and to an EMAC timeslice experiment representing the year 2000 to investigate precipitation in the South Asia Monsoon period. The EMAC simulation generally overestimates precipitation in South Asia during the local summer and winter seasons compared to observations, and also the global precipitation intensity, which is calculated as summer minus winter difference. This bias in precipitation intensity results in an overestimation of the global monsoon domains, which are areas that exceed a precipitation intensity of 2.5 mm per day. Compared to the CMIP5 historical simulations, not only the CMIP5 multi-model mean but also each individual model is more skillful in terms of pattern correlation index. Possible reasons for biases in the EMAC simulation could for example arise from biases in circulation or the representation of clouds. The simulation of the 850 hPa low-level wind was better represented than the precipitation intensity, although some biases compared to meteorological reanalysis exist. Diagnostics have been newly developed and implemented into the ESMValTool to examine the representation of Cloud Radiative Effects (CRE) as external solar radiation is the main driver for monsoon. Deviations from observations are found in particular for the simulated shortwave radiation, which could be related to problems in the representation of low-level clouds. The biases found in the particular EMAC simulation evaluated here could partly be due to the boundary conditions used, in particular the prescribed sea surface temperatures (SST) that are taken from a CMIP5 model simulation with the CMCC model. In addition, a coupled ocean could possibly partially compensate for the biases in precipitation. Additional work is required to investigate this further. For example, an EMAC simulation with observed SSTs or a coupled ocean could be evaluated to better understand the reasons for the biases found here.

Contents

1	Introduction	3
1.1	Background and Motivation	3
1.2	Structure of the Thesis	4
2	Scientific Background	4
3	Model Simulations	5
3.1	Simulations from the Coupled Model Intercomparison Project (CMIP5)	5
3.2	ECHAM/MESSy Atmospheric Chemistry (EMAC) model	7
4	Earth System Model Evaluation Tool (ESMValTool) and Diagnostics	9
4.1	Earth System Model Evaluation Tool (ESMValTool)	9
4.2	Monsoon Diagnostics and Observations for Model Evaluation	9
4.3	Diagnostics for the Cloud Radiative Effects	10
5	Results	12
5.1	Precipitation in South Asia	12
5.1.1	Evaluation of Daily Mean Precipitation in the CMIP5 Multi-Model Mean	12
5.1.2	Evaluation of Daily Mean Precipitation in the EMAC ACCMIP simulation	14
5.2	Global Precipitation Intensity and Domains	16
5.2.1	Evaluation of Global Precipitation Intensity and Domains in the CMIP5 Multi-Model Mean	16
5.2.2	Evaluation of Global Precipitation Intensity and Domains in the EMAC ACCMIP simulation	19
5.3	Possible Reason for Biases in the EMAC ACCMIP simulation	22
5.3.1	Observational Uncertainty	22
5.3.2	Biases in the Prescribed Sea Surface Temperature Dataset	23
5.3.3	Prescribed Sea Surface Temperatures rather than Coupled Mode	23
5.3.4	Biases in the Simulation of 850 hPa Low-Level Winds	26
5.3.5	Biases in Radiation and Cloud Parameterization	28
5.3.6	Other Influences	34
6	Summary and Outlook	35
7	Acknowledgements	37
8	References	39

1 Introduction

1.1 Background and Motivation

The ability to understand and project future climate is fundamental to society. The Intergovernmental Panel on Climate Change (IPCC) Fifth Assessment Report (AR5) concluded that continued emissions of greenhouse gases would cause further warming (IPCC, 2013). An important component of the earth's climate system is the global monsoon, determining around half of the world's population life due to its major impact on food and energy security. Strong sub-seasonal variations can cause extreme events, for example the Pakistan flood in 2010, that require forewarning in order to better cope with the consequences (Sperber et al., 2012). Apart from its strong impact on society, monsoon plays a major role for the atmospheric general circulation and in linking external radiative forcing to atmospheric circulation (Wang et al., 2011). Monsoon is primarily determined by external solar forcing (Sperber et al., 2012), but also by cloud radiative effects, orography and other factors. The absorbance and reflection characteristics of clouds and their global distribution play a key role not only for monsoon but also in the understanding of the climate change in general (IPCC, 2013).

In order to better understand past and future changes in the earth's climate and to provide reliable climate projections, complex Earth system models (ESMs) are developed. The performance of the models can be tested by testing their ability to reproduce past and present-day climate in comparison to observations. To facilitate routine benchmarking and evaluation of single or multiple ESMs, either against predecessor versions, a wider set of climate models or observations, the Earth System Model Evaluation Tool (ESMValTool) is developed at DLR-IPA in collaboration with international partners.

The goal of this thesis is to evaluate the representation of the South Asian Monsoon in ECHAM/MESSy Atmospheric Chemistry Model (EMAC, Jöckel et al., 2006) in comparison to observations and models participating in the 5th Phase of the Coupled Model Intercomparison Project (CMIP5, Taylor et al. (2012)). Hereby, a set of existing monsoon diagnostics from the ESMValTool is applied to an EMAC and the CMIP5 simulations. To understand possible deviations compared to the observations, basic features of the general circulation are evaluated by looking at the surface winds. In addition, new diagnostics to evaluate the Cloud Radiative Effects (CRE) diagnostics are developed and implemented into the ESMValTool to assess the performance of EMAC in comparison to observations.

1.2 Structure of the Thesis

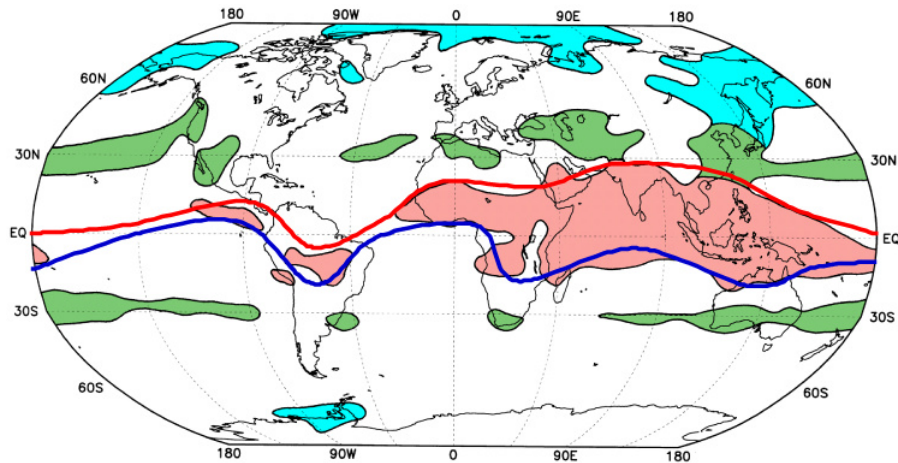
This thesis includes six chapters. Chapter 2 gives a brief overview of the scientific background for monsoon. Chapter 3 introduces the climate models that have been used in this work. Chapter 4 briefly explains the Earth System Model Evaluation Tool (ESMValTool) as well as all diagnostics that have been applied. The results are presented in Chapter 5 complemented with a discussion of possible reasons for biases. Chapter 6 summarizes this work and gives an outlook.

2 Scientific Background

Global Monsoon is determined by seasonal changes in atmospheric circulation and precipitation associated with asymmetric heating of land and sea. The asymmetric heating is due to the different heat capacity of land and sea that causes land surfaces to heat faster. In Southeast Asia, the intense solar heating in late spring and early summer leads to a heat low over the landmass that induces land-sea thermal and pressure gradients. As a consequence, cross-equatorial low-level winds develop and transport an increased amount of moisture, which is further boosted by the strong coupling between diabatic heating and circulation (Sperber et al., 2012). While the annual variation of solar radiation is both a necessary and sufficient condition for the development of monsoon, land-sea thermal contrast itself is critical for the location and strength but neither necessary, nor sufficient. Thus monsoon is a global phenomenon since solar forcing as its fundamental driver is affecting the whole planet (Wang et al., 2011). As a result, massive rainfalls during the monsoon season occur while their spatial distribution is mainly determined by the orographic structure of the Asian landmass. Especially the Western Ghats, foothills of the Himalayas and the Burmese coast as well as the Philippines provide anchor points, where observed rainfall is concentrated (Sperber et al., 2012).

Figure 1 illustrates monsoon as a global phenomenon. Whereas this thesis focuses on South Asia, monsoon regions are also present in North Australia, West Africa and North as well as South America.

When investigating monsoon and its year-to-year variation, it is not appropriate to use the normal calendar year as time period. Since both northern and southern hemisphere has its monsoon seasons taking place during a different period (May to October in the northern hemisphere and November to April in the southern hemisphere), it makes sense to define a monsoon year starting from April in order to capture both peaks.



The red, green, and blue areas indicate the tropical, subtropical, and temperate-frigid monsoons, respectively. The red and blue thick lines represent the ITCZ in summer and winter, respectively. (Li, J., and Q. Zeng, 2005)

Figure 1: Geographical extent of the global surface Monsoons.

3 Model Simulations

3.1 Simulations from the Coupled Model Intercomparison Project (CMIP5)

The World Climate Research Programme’s (WCRP) Coupled Model Intercomparison Project Phase 5 (CMIP5) is a set of coordinated climate model experiments with more than 20 modeling groups from all over the world participating with over 50 different model versions. The focus is on major gaps in understanding of past and future climate changes through assessing model differences in poorly understood feedbacks associated with the carbon cycle and clouds on the one hand. On the other hand, a major issue is to examine the predictive capabilities of forecast systems on decadal time scales (Taylor et al., 2012).

Figure 2 provides a schematic overview of the CMIP5 long-term experiments with a central core of simulations that is surrounded by tier 1 and tier 2 experiments. The core consists of an Atmospheric Model Intercomparison Project (AMIP) experiment where sea-surface temperatures are prescribed from observations, a coupled control experiment and a coupled historical experiment which is forced by observed atmospheric

composition changes. The Representative Concentration Pathways (RCP) describe different emission scenarios that are based on low (2.6 W m²) to high (8.5 W m²) increases in the radiative forcing in the year 2100 compared to preindustrial conditions. Tier 1 and 2 experiments provide a more detailed analysis of the core simulations such as carbon cycle feedback experiments or aerosol forcing.

In this thesis, the climatological mean (1995-2005) of the historical CMIP5 simulations are compared to observations averaged over the same time period.

CMIP5 models are used in the first step to reproduce existing figures – for example Figure 9.5 of IPCC AR5 (IPCC, 2013) providing an ability to compare to published figures.

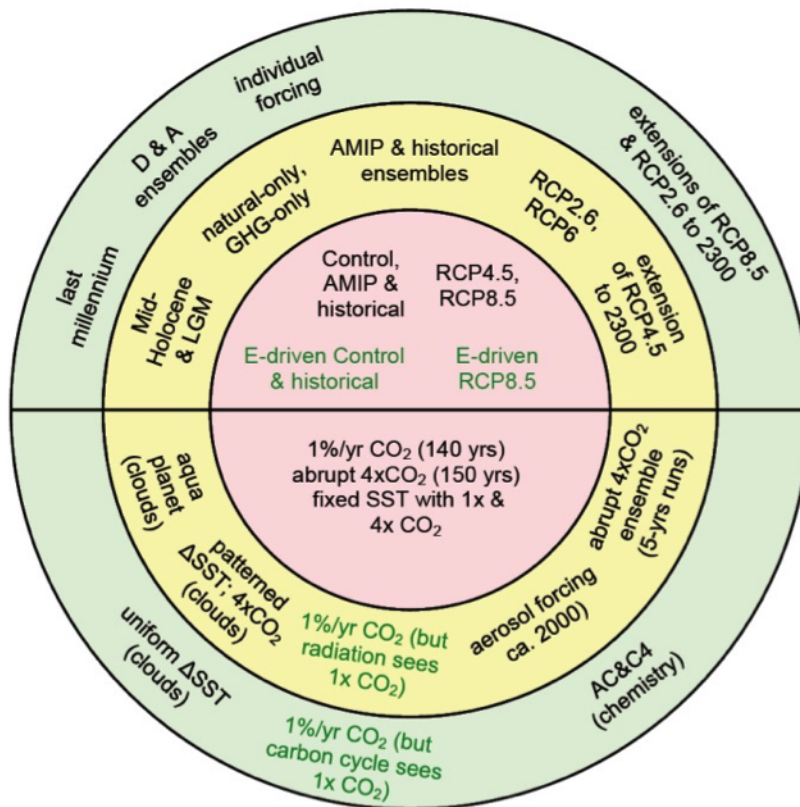


Figure 2: Schematic structure of the CMIP5 long-term experiments (from Taylor et al., 2012).

3.2 ECHAM/MESSy Atmospheric Chemistry (EMAC) model

The ECHAM/MESSy Atmospheric Chemistry (EMAC) model is a numerical chemistry and climate simulation system that includes various submodels describing atmosphere processes and their interactions with oceans, land and human influences based on the Modular Earth Submodel System (MESSy) interface that couples submodels to a general circulation model (Röckner et al., 2006). The core atmospheric model is the 5th generation European Centre Hamburg general circulation model (ECHAM5) including more than 30 submodels with different functions.

Name	Resolution	Analysed time period	Running mode
Eval2	T42L90MA	1999-2009	Nudged, coupled
QCTM	T42L90MA	1999-2007	Nudged, QCTM
TS2000	T42L90MA	10 years under 2000 conditions	Free-running timeslice, coupled
ACCMIP	T42L90MA	10 years under 2000 conditions	Free-running timeslice, coupled

Table 1: Summary of the different EMAC simulations. In this thesis, the free-running ACCMIP timeslice experiment is used over a period of 10 years simulated under 2000 conditions (from Klinger et al., 2014).

From the four EMAC simulations that were evaluated in Klinger et al. (2014), see Table 1, in this thesis the EMAC ACCMIP timeslice experiment is used. It was performed in support of the Atmospheric Chemistry and Climate Model Intercomparison Project (ACCMIP) and has been evaluated in a number of papers (Fiore et al., 2012; Klinger et al., 2014; Lamarque et al., 2013; Naik et al., 2013; Silva et al., 2013; Stevenson et al., 2013; Voulgarakis et al., 2013; Young et al., 2013). The EMAC-ACCMIP timeslice experiment was run in a free-running mode over a period of 10 years under 2000 conditions. Hereby, monthly mean sea surface temperatures (SSTs) and sea ice concentrations (SICs) from the historical CMIP5 experiment carried out with the CMCC climate model are prescribed as a 10-year climatological mean around the base year 2000. The TS2000 experiment uses observed SSTs and SICs and slightly different emission inventories. More details of the EMAC ACCMIP simulation can be found in Klinger et al. (2014). Table 2 summarizes the key figures of the setup.

Resolution	T42 (2.8 · 2.8 degrees), L90 (up to 0.01hPa)
Anthropogenic and biomass burning emissions	Based on CMIP5 dataset (Lamarque et al., 2010) T42L90MA
Lightning NO_x	Calculated interactively based on the Grewe et al. (2001) parameterization
Natural emissions	Interactive isoprene and soil NO_x , constant emissions of DMS, volcanic SO_2 , biogenic CO and NMHCs
Long-lived species (including methane)	Prescribed surface concentrations based on AGAGE (2000) and rescaled according to CMIP5 concentration data (past and future)
SST/SIC	Decadal means from the CMCC climate model simulations in CMIP5
Radiation couplings	Online CO_2, CH_4, N_2O, O_3 , CFCs, water vapor. Climatological aerosol
Chemistry	179 gas phase reactions (tropo- and stratospheric), 61 photolysis reactions, 10 PSC reactions, 26 heterogeneous reactions, 3 aqueous-phase reactions.
Convection	Tiedtke scheme with Nordeng closure
Clouds	Standard ECHAM5 module based on Lohmann and Roeckner (1996), PSC based on the model by Kimer et al. (2011).
Aerosol	No interactive aerosol

Table 2: Key figures of the EMAC ACMMIP setup.

4 Earth System Model Evaluation Tool (ESMValTool) and Diagnostics

4.1 Earth System Model Evaluation Tool (ESMValTool)

As discussed in the introduction, it is important to continuously evaluate and improve the performance of climate models. To facilitate routine benchmarking and evaluation of single or multiple ESMs, the Earth System Model Evaluation Tool (ESMValTool) is developed at DLR-IPA in collaboration with international partners. The tool allows to easily compare new simulations to existing runs and observations as well as quick production of standard diagnostic plots and output diagnostic variables.

The ESMValTool is based on Python scripts that call NCAR Command Language (NCL) and other open source languages like R.

One of the advantages of the ESMValTool is that it can easily read in multiple model simulations and observations that are archived in CMIP format. This is done via the namelist structure that then calls NCL diagnostics scripts that process the data and further pass it to plotting routines. Reformat scripts ensure that variables have the right format and units according to Climate Model Output Rewriter (CMOR) standards.

In this work the Monsoon diagnostics of the ESMValTool have been applied to the EMAC ACCMIP simulation and the CMIP5 model simulations, and additional new diagnostics to evaluate CRE have been implemented into the ESMValTool and applied to EMAC ACCMIP.

4.2 Monsoon Diagnostics and Observations for Model Evaluation

This section gives an overview of the South Asia Monsoon (SAMonsoon) diagnostics that are implemented in the ESMValTool. Each diagnostic is referred to as a plot type, which on the technical side corresponds to a single file that will generate a restricted set of figures.

- *SAMonsoon_precip_basic*: Mean and standard deviation of precipitation in South Asia across all years for each model as well as the multi-model mean. This plot

type also outputs the difference of the mean and standard deviation with respect to a reference model.

- *SAMonsoon_global_domain*: Plots the local summer minus winter average globally and also produces a plot that contours precipitation only above a cut off level to identify monsoon domain areas
- *SAMonsoon_wind_basic*: Mean and standard deviation of 250hPa and 850hPa low-level winds in South Asia across all years for each model as well as the multi-model mean. This plot type also outputs the difference of the mean and standard deviation with respect to a reference model.
- *SAMonsoon_precip_seasonal*: Produces climatology, seasonal anomalies and interannual variability of monsoon precipitation in South Asia.
- *SAMonsoon_wind_seasonal*: Various monsoon indices computed over the monsoon season (JJAS) and as annual cycles.

These diagnostics are included in two different namelists with one calling the diagnostic with monthly data and the other one with daily data. In this thesis, diagnostics 1-3 have been used with the monthly mean data namelist.

For precipitation diagnostics, the Global Precipitation Climatology Project (GPCP) observational dataset GPCP-SG has been used as reference. GPCP-SG is the combined monthly Satellite Gauge (SG) data set for precipitation estimates based on a $2.5^{\circ} \times 2.5^{\circ}$ grid. The GPCP combined precipitation data were provided by the NASA/Goddard Space Flight Center's Laboratory for Atmospheres, which develops and computes the dataset as a contribution to the GEWEX Global Precipitation Project (Huffman et al., 1997). To investigate observational uncertainty, the Tropical Rainfall Measuring Mission (TRMM) data (Huffman et al., 2007) is used as an alternative dataset.

Simulated winds are compared to the European Reanalysis (ERA) ERA-Interim reanalysis dataset with a spatial resolution of about $0.75^{\circ} \times 0.75^{\circ}$, which was produced by the European Centre for Medium Range Weather Forecasts (ECMWF). The data is based on geostationary satellite scatterometer measurements (Dee et al., 2011).

4.3 Diagnostics for the Cloud Radiative Effects

Unlike monsoon diagnostics, diagnostics for cloud radiative effects (CRE) were not included in the ESMValTool so far. To understand possible biases, CRE diagnostics

have been developed and implemented into ESMValTool to assess the performance of EMAC in comparison to observations. Hereby, the “Clouds And Earth’s Radiant Energy Systems Energy Balanced and Filled” dataset (CERES-EBAF) has been used as observations in the period from 1995 to 2005. To evaluate the effects of clouds, top of the atmosphere (TOA) data for longwave and shortwave radiation under both clear sky and all sky conditions have also been calculated. CREs are defined as the difference between clear sky and all sky conditions.

Two different diagnostics have been implemented into the ESMValTool:

- The bias between models and observations in the global distribution of CREs for both shortwave and longwave radiation and the net effect that is defined as the sum of both CREs. This is outputted as a contour plot indicating areas of misrepresentation of CRE in the models evaluated. For CMIP5 models, a multi-model mean has been calculated.
- Zonal mean plots containing both model and observational data to compare the absolute values averaged over the longitudes.

These diagnostics can reproduce Figure 9.5 of the IPCC AR5 (Flato et al., 2013) and have been first applied to the CMIP5 models and multi-model mean for comparison, and have been used in a second step to evaluate the EMAC ACCMIP simulation.

The CERES-EBAF satellite observations provide monthly mean TOA shortwave, longwave and net fluxes under both clear sky and all sky conditions based on a one-degree resolution. One of its key limitations is that clear sky fluxes can only be determined when the satellite catches cloud free regions. However, the models simply remove clouds in their simulations to calculate clear sky condition, which can lead to differences. Nevertheless, especially due to its extensive validations through ground-based measurements, CERES-EBAF provides a very good reference dataset (Loeb et al., 2014).

5 Results

In this section the results of the thesis are presented, focusing first on the EMAC evaluation for precipitation in the South Asian Monsoon region compared to the CMIP5 multi-model mean (Section 5.1) and the global precipitation intensity and domains (Section 5.2). Section 5.3 then discusses possible reasons for the detected differences between the EMAC ACCMIP simulation and observations.

5.1 Precipitation in South Asia

Precipitation is besides typical circulation patterns one of the most important characteristics of the monsoon. To capture and evaluate it, an existing diagnostic of the ESMValTool is used that calculates and plots the mean and standard deviation of the daily mean precipitation during the monsoon season across all years for each model based on monthly mean output. Furthermore, the difference with respect to observational data is calculated to assess the performance of the models. In order to assess the amount of increased rainfall during the monsoon season the difference between the local summer from June to September (JJAS) and the local winter from November to February (NDJF) is calculated.

5.1.1 Evaluation of Daily Mean Precipitation in the CMIP5 Multi-Model Mean

As a first step, the above-mentioned diagnostic was applied to the individual CMIP5 models and the CMIP5 multi-model mean. Figure 3 shows the climatological mean monthly mean precipitation (mm/day) for the monsoon season (June to September (JJAS), left) and the local winter (November to February (NDJF), right) for the GPCP-SG satellite observations (upper row), the CMIP5 multi-model mean (middle row), and the difference between the CMIP5 multi-model mean (MMM) and the observations (bottom row). The observations are averaged over the period 1995 to 2005 and the CMIP5 models over 1995 to 2004. The difference is due to missing data for one of the models but has no measurable effect on the results.

The observed geographical pattern of daily mean precipitation is very well represented in the CMIP5 MMM with a correlation coefficient of 0.9 in both local summer and

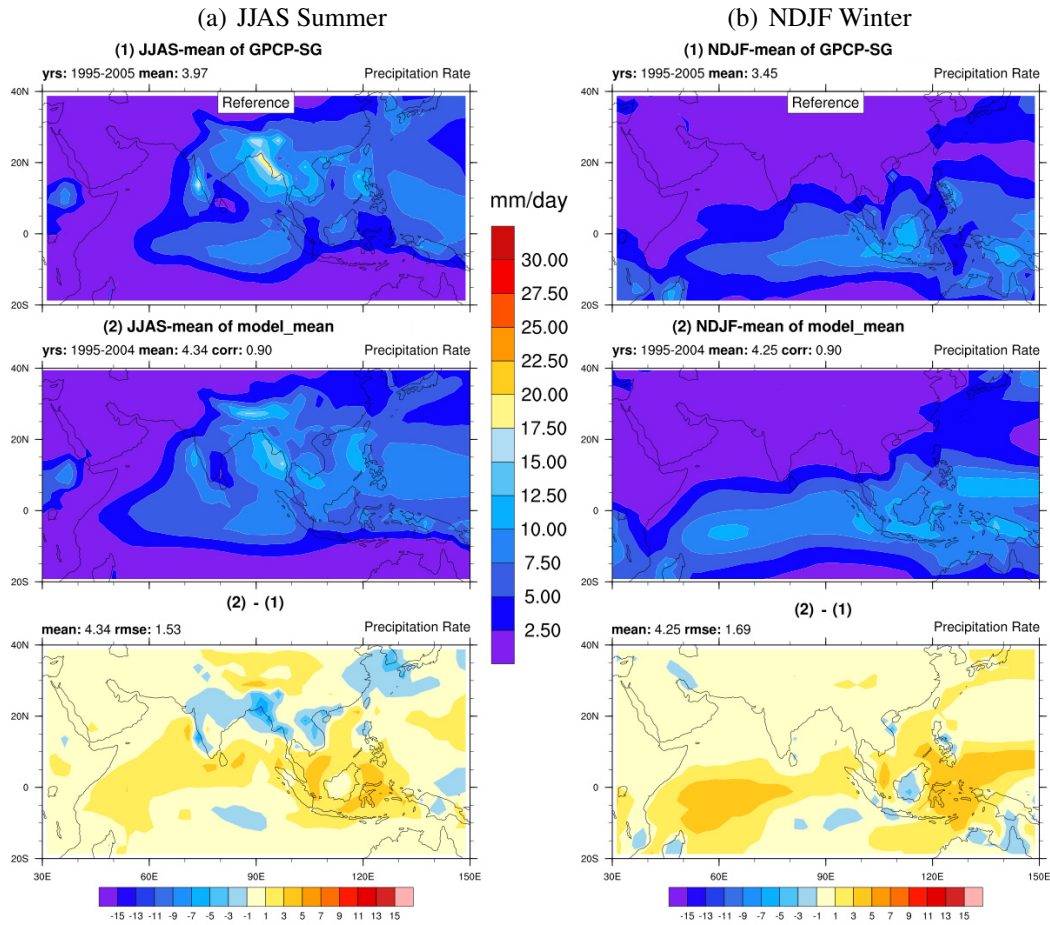


Figure 3: Climatological mean monthly mean precipitation in South Asia for JJAS summer (a) and NDJF winter season (b). (1) GPCP-SG Observations (2) CMIP5 multi-model mean and below the difference between multi-model mean and observations.

local winter. The CMIP5 MMM thereby outperforms every single model for the pattern correlation skill metric (not shown). The CMIP5 MMM captures both precipitation maxima along the Indian and the Indochina west coast but underestimates the intensity of rainfall. In contrast, precipitation over most of the tropical western and central Indian Ocean as well as large parts of South East Asia is overestimated. As a consequence, the total mean precipitation is 4.3 mm/day and hence higher than the observed value of 4.0 mm/day. In winter, the overestimation of daily mean precipitation is even stronger than during the monsoon summer season. Especially over the maritime continent as well as the western part of the Indian Ocean, there is too much precipitation.

5.1.2 Evaluation of Daily Mean Precipitation in the EMAC ACCMIP simulation

Applying the same diagnostics to the EMAC ACCMIP simulation shows that the correlation index calculated against GPCP-SG satellite data is significantly lower (0.75) than the CMIP5 multi-model mean index (0.90) in the summer season (Figure 4, left) and winter (Figure 4, right). A comparison to the individual CMIP5 models (not shown) reveals that the correlation from EMAC ACCMIP is lower than the lowest one of the CMIP ensemble (EC-EARTH, 0.79).

Although the two summer precipitation maxima at the Indian and Indochina west coast are simulated as areas with increased precipitation in EMAC ACCMIP, these areas are no clear maxima in the simulation. Overall there is a distinct overestimation of precipitation over the maritime continent with relative errors of around 50% as well as over the western part of the Indian Ocean and the Chinese highlands. Compared to the CMIP5 multi-model mean, the overestimation of daily mean precipitation in the summer and winter monsoon seasons is significantly stronger. Nevertheless, the observational rainfall maxima at the Indian and Indochina west coast are less underestimated than in the CMIP5 MMM.

Excessive rainfall is simulated over the western Indian Ocean to the east of Africa during NDJF, which does not correspond to observed data. Moreover, precipitation is heavily overestimated to the north of Indonesia and parts of the maritime continent. This distinct overestimation produces a relative error of more than 65%. In addition, precipitation over the Indian Ocean south of India as well as northern Australia is underestimated. Areas of very low rainfall daily mean precipitation ($<2,5$ mm/day) on the other hand are very well simulated by EMAC ACCMIP.

Areas of very low rainfall daily mean precipitation ($<2,5$ mm/day) on the other hand are very well simulated by EMAC ACCMIP.

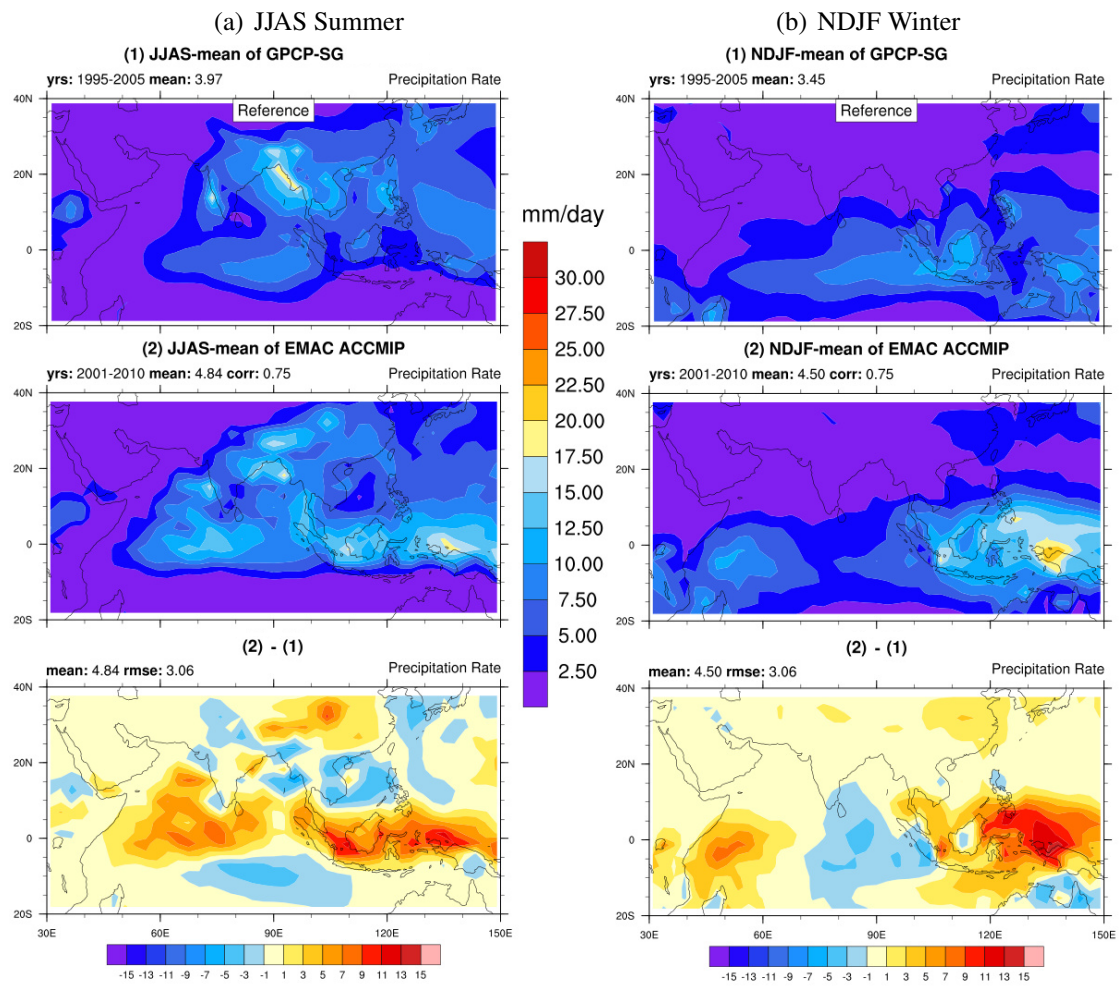


Figure 4: As Figure 4, but using the EMAC ACCMIP simulation.

5.2 Global Precipitation Intensity and Domains

The evaluation of the global precipitation intensity and the monsoon domains give additional insights of how well models perform compared to observations. To better capture the intensity of the monsoon, the global precipitation intensity is calculated from the difference between the local summer minus the local winter mean.

$$pr_{GlobalIntensity} = pr_{Summer} - pr_{Winter} \quad (5.2.1)$$

The global precipitation intensity is then used to calculate the global monsoon domains, defined by those areas where the precipitation intensity exceeds 2.5 mm/day. This allows an assessment of the general ability of models to simulate monsoon on a global scale.

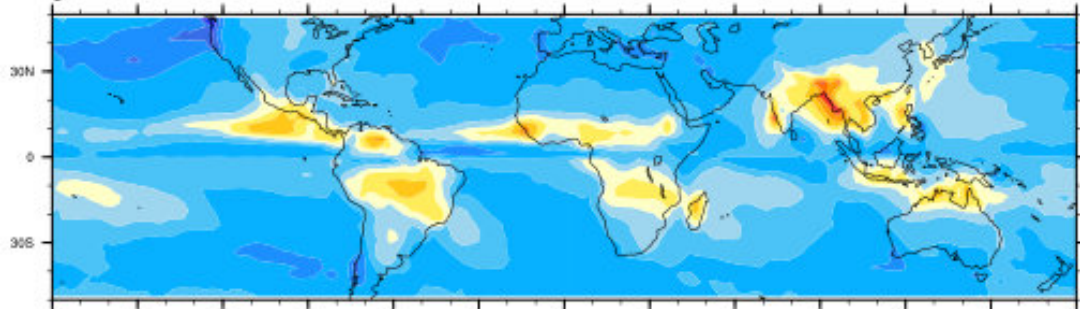
$$GlobalMonsoonDomain : pr_{Summer} - pr_{Winter} > 2.5mm/day \quad (5.2.2)$$

5.2.1 Evaluation of Global Precipitation Intensity and Domains in the CMIP5 Multi-Model Mean

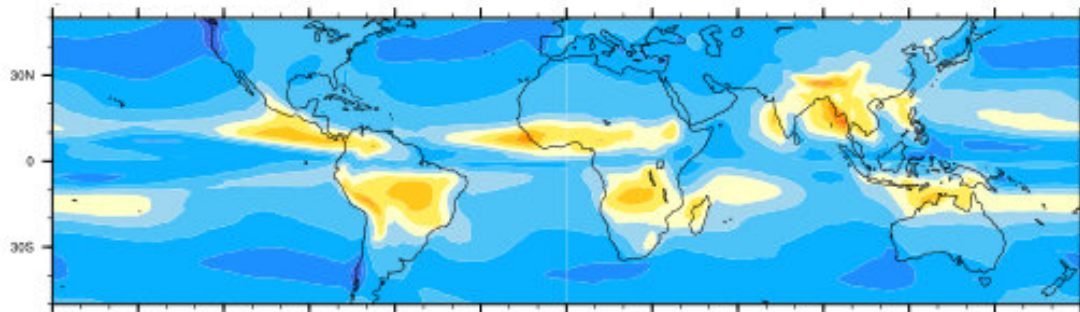
The CMIP5 multi-model mean captures the precipitation intensity very well compared to the GPCP-SG observations (Figure 5). There is a slight overestimation of roughly 4 mm/day over the Gulf of Guinea and parts of the South American west coast but overall the deviation is very low. Slight underestimation occurs at the Indochina west coast as well as over Indonesia and Micronesia. Biases in the summer and winter period that have been shown in Figure 3 are partly compensated which leads to an overall good representation of global precipitation intensity (Figure 5) and the global monsoon domains (Figure 6). However, domains are still slightly overestimated all over the Earth with only a few spots of underestimation that are red colored in the plot showing the difference between the multi-model mean and observations.

(a) GPCP-SG Observations

yrs: 1995-2005



(b) CMIP5 MMM



(c) CMIP5 MMM - Observations

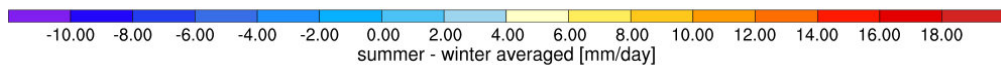
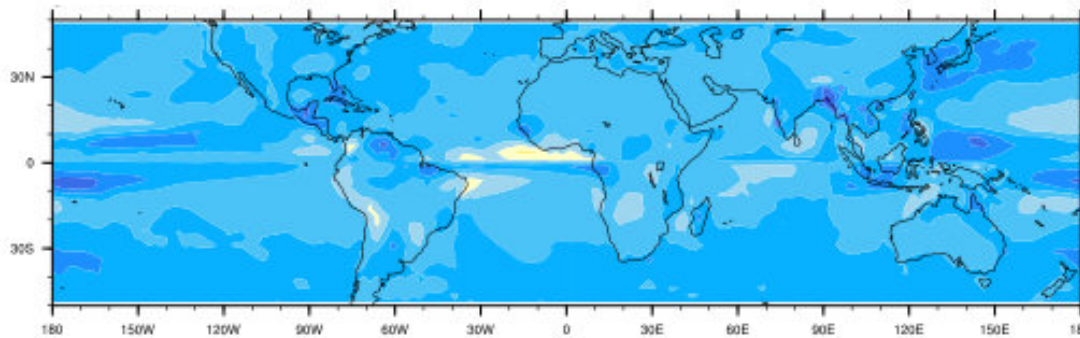
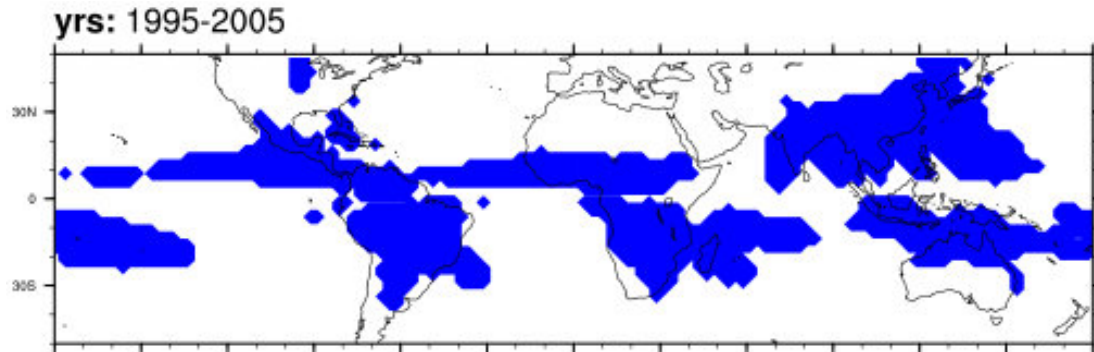
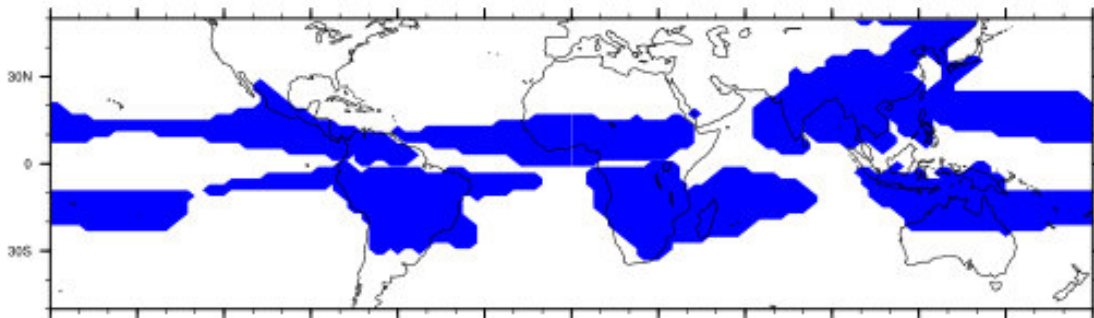


Figure 5: Global Monsoon Intensity – Mean summer minus winter averaged.

(a) GPCP-SG Observations



(b) CMIP5 MMM



(c) CMIP5 MMM - Observations

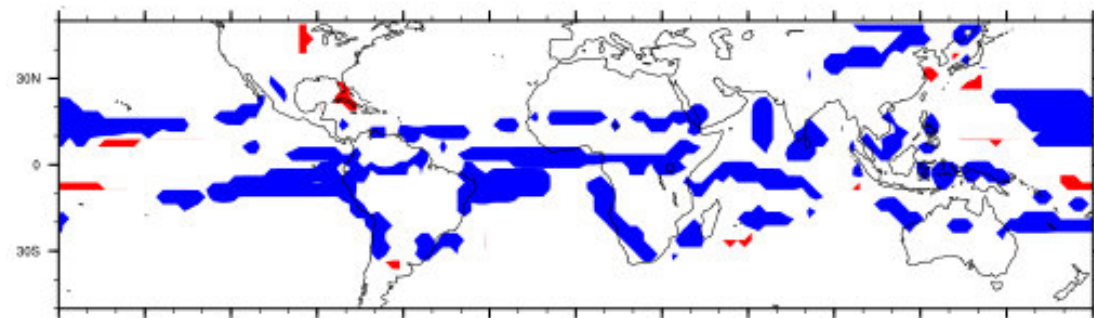


Figure 6: Global Monsoon Domains. Bottom plot shows differences between the CMIP5 multi-model mean and GPCP-SG operations, where blue spots indicate over-estimation in domains and red spots indicate underestimation.

5.2.2 Evaluation of Global Precipitation Intensity and Domains in the EMAC ACCMIP simulation

The global precipitation intensity is clearly overestimated in the EMAC ACCMIP simulation (Figure 7). Analogously to the CMIP5 multi-model mean, there is a distinct overestimation of rainfall over the Gulf of Guinea along the South Atlantic Ocean reaching almost to South America, yet even more intense in EMAC. In addition, precipitation intensity over Brazil is too strong. However, the most striking differences are found in the region around India and South East Asia where both over- and underestimation of rainfalls occur in the EMAC simulation compared to GPCP-SG data. While the precipitation intensity over the Indian Ocean south of India and parts of the maritime continent is clearly too high, the amount of rainfall over the Philippine Sea as well as parts of Indonesia is fairly underestimated.

In contrast to the CMIP5 multi-model mean, errors in both JJAS and NDJF periods do not compensate each other but contribute to the biases in India and South East Asia. It is interesting to notice that negative biases mainly occur in this area which may be either due to better compensation of errors or a better performance in general in the other regions.

Based on the global monsoon precipitation intensity errors, monsoon domains are overestimated in general as in the CMIP5 multi model mean. However, especially in the South East Asia area the overestimation is stronger than in the CMIP5 multi-model mean. On the other hand, the monsoon domain over Indonesia is slightly underestimated compared to satellite observations.

Neither the simulation of the JJAS monsoon summer season nor the NDJF winter season are the reason for the overestimation of monsoons to a special degree. In fact, the overestimation in the domains (figure 8) arises from errors in both seasons that add up to the simulated pattern. Although there are areas of clear overestimation that also compensate each other, the large relative errors of up to 65% and more facilitate to trigger the 2.5 mm per day threshold. As a result, monsoon domains of different continents are connected and reach from North America via Africa and the Indian Ocean to the maritime continent in South East Asia.

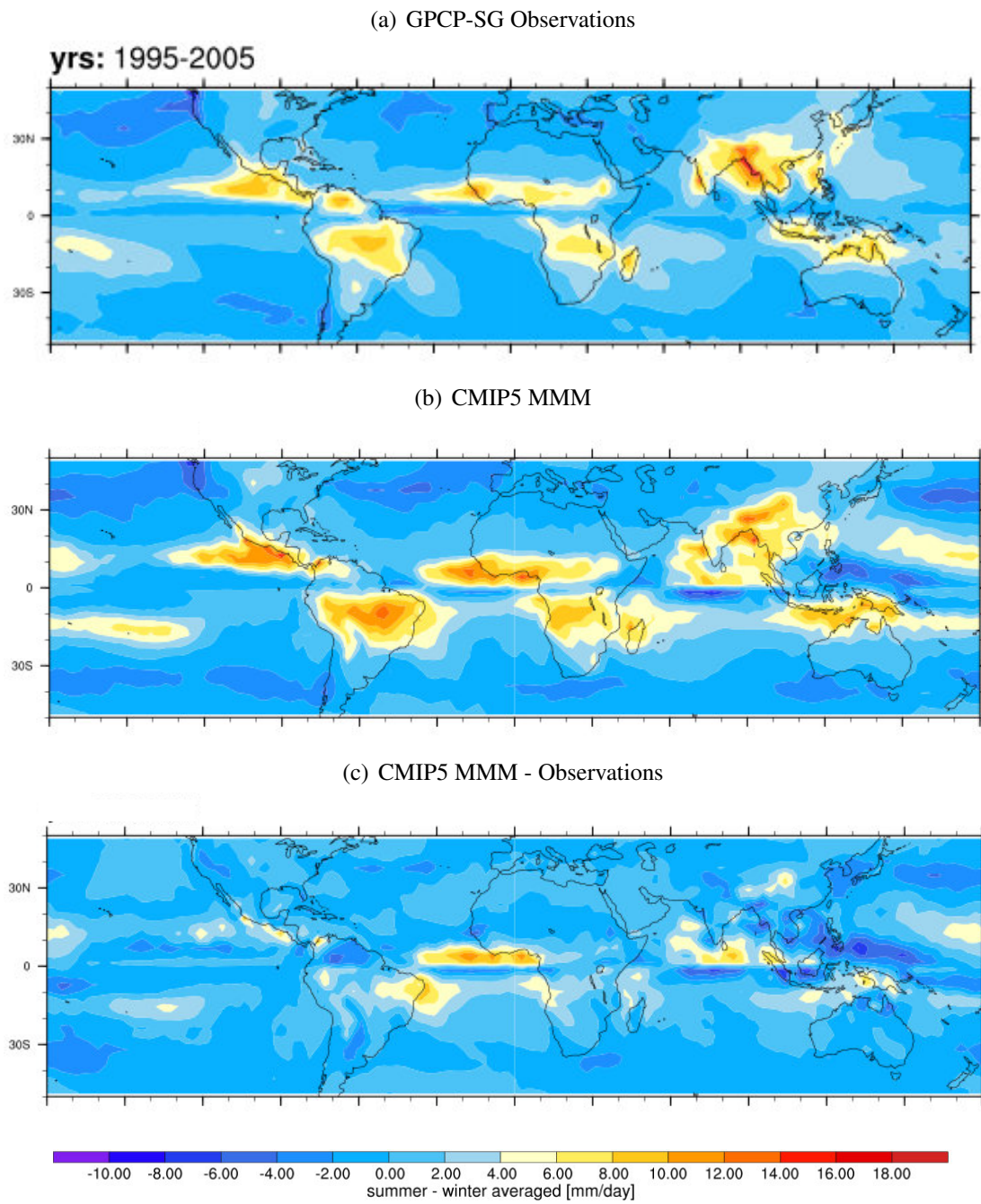
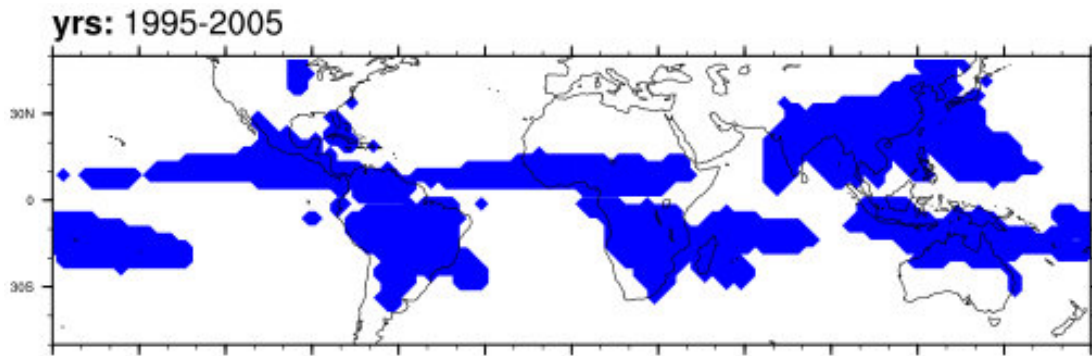
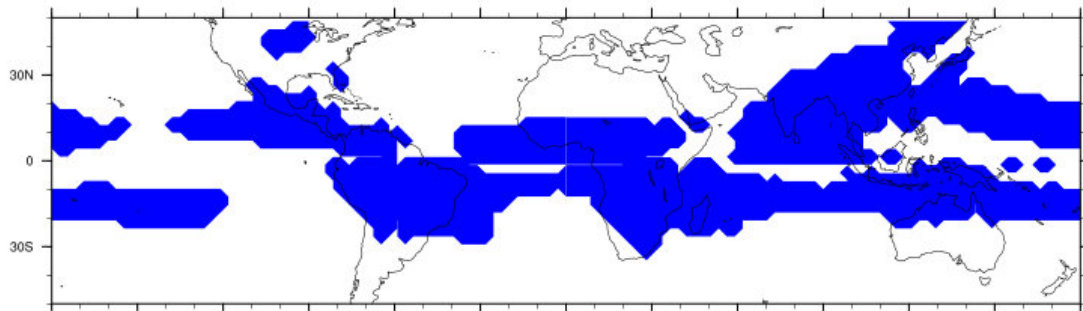


Figure 7: As for figure 5, but showing the EMAC ACCMIP simulation.

(a) GPCP-SG Observations



(b) CMIP5 MMM



(c) CMIP5 MMM - Observations

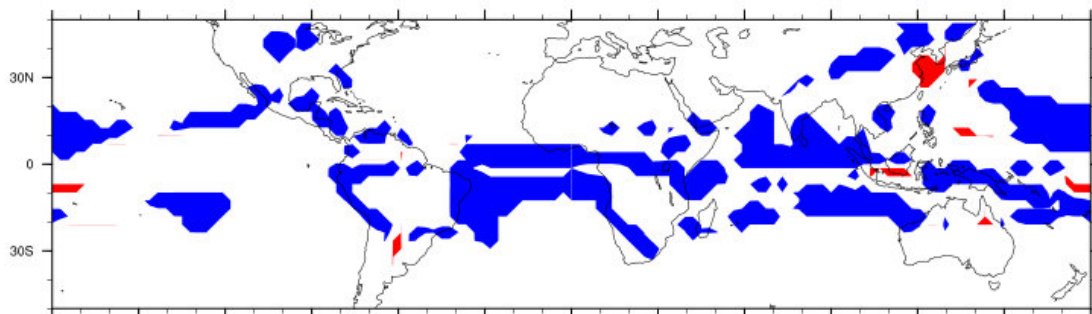


Figure 8: As for figure 6, but showing the EMAC ACCMIP simulation.

5.3 Possible Reason for Biases in the EMAC ACCMIP simulation

In order to better understand the performance of the simulation, it is inevitable to identify possible reasons for biases. As monsoon is a coupled phenomenon there are many sources for errors that can lead to biases in the simulation of precipitation, some of them being discussed below.

5.3.1 Observational Uncertainty

To assess the performance of climate model simulations, the outcome is compared to observational data. However, it is important to consider observational uncertainty. This is evident when comparing two different observational datasets to each other. To investigate this, the Tropical Rainfall Measuring Mission (TRMM) data (Huffman et al., 2007) is used as an alternative dataset. Figure 9 shows the differences between the GPCP-SG observations used as the reference dataset in previous comparison and the TRMM satellite data for the JJAS summer in South Asia. In particular over the India and Indochina west coast daily mean precipitation in TRMM is clearly higher than in GPCP-SG with deviations up to 5 mm/day. Especially at the Indian west coast deviations to GPCP-SG of TRMM and the EMAC ACCMIP simulation lie within the same magnitude.

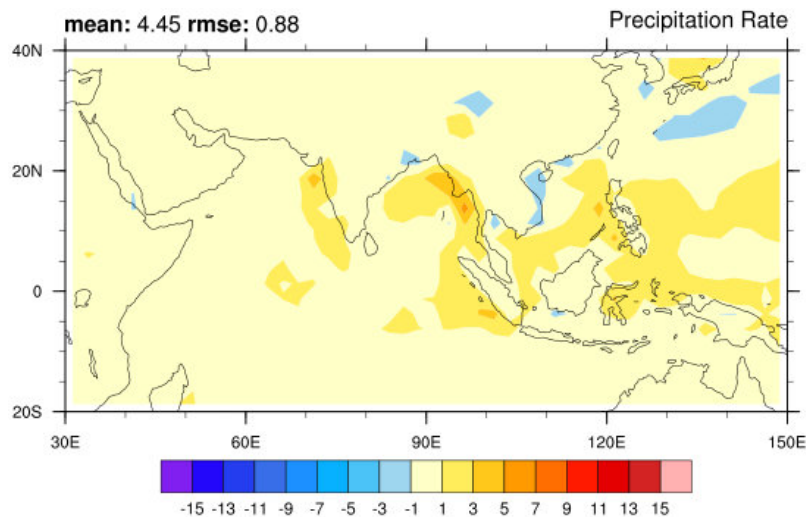


Figure 9: Differences between GPCP-SG and TRMM observations during JJAS summer in South Asia in units mm/day.

In general, the mean precipitation in South Asia is significantly higher for TRMM while the correlation index of 0.98 compared to GPCP-SG indicates also some uncertainty in the pattern. This can lead to general biases in the estimation of the intensity of precipitation but not explain strong local deviations of up to 13 mm/day over the maritime continent in EMAC ACCMIP.

5.3.2 Biases in the Prescribed Sea Surface Temperature Dataset

A second possible reason for biases in the precipitation could be biases in the prescribed SST and SIC dataset. In the EMAC ACCMIP simulation, monthly mean SSTs and SICs are prescribed as a 10-year climatological mean around the base year 2000 using the historical CMIP5 experiment carried out with the CMCC climate model. Figure 10 from Klinger et al. (2104) shows the simulated annual mean SSTs in CMCC and the differences compared to HadISST observations.

SSTs in the CMCC simulation in the area of the maritime continent are underestimated compared to observations by around 1.2 K. Comparing this with the excess of rainfall over the maritime continent, similar error pattern can be found meaning that areas of underestimated SSTs have a tendency to match with areas with overestimated precipitation and vice versa for areas of overestimated SSTs. Furthermore SSTs at the Indian and Indochina west coast are too high by around 0.6 K which may be a possible reason for the underestimation of precipitation there in the EMAC ACCMIP simulation.

However, as figure 10 shows the annual mean sea surface temperature but precipitation plots in South Asia are based on the JJAS season, this discussion is only a rough and qualitative indicator that biases in SSTs could be related to biases in precipitation evaluated before.

5.3.3 Prescribed Sea Surface Temperatures rather than Coupled Mode

Apart from errors in the sea surface temperatures used, there is a second aspect that can contribute to biases compared to observations when simulating precipitation. According to Sperber et al. (2013), in coupled models errors in simulating sea surface temperatures partly compensate precipitation biases leading to a better result than for models without coupling. Hence the use of prescribed SSTs could lower the model performance due to less error compensation between precipitation and SSTs.

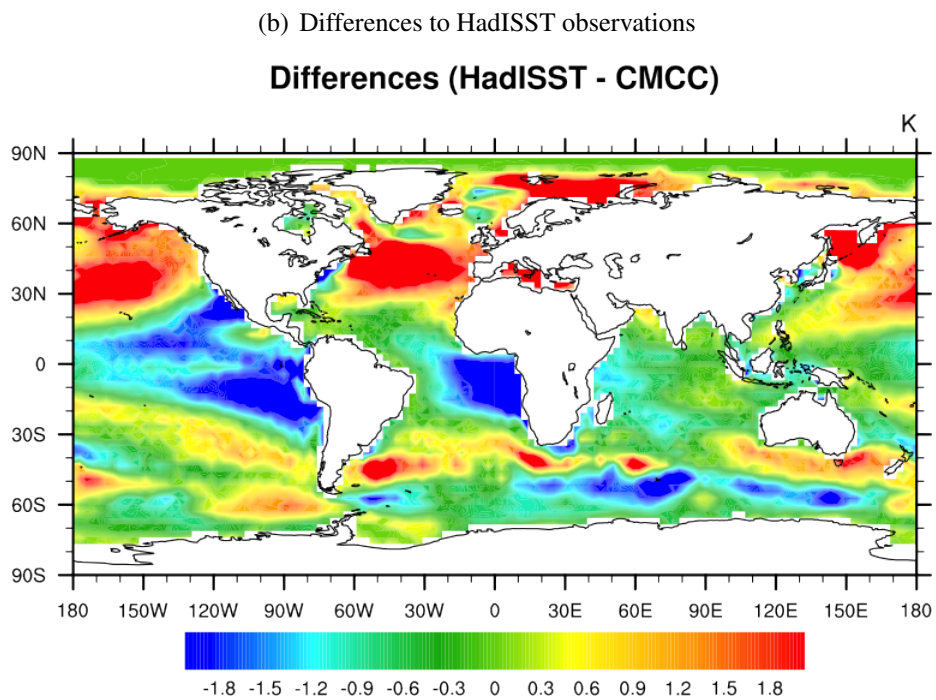
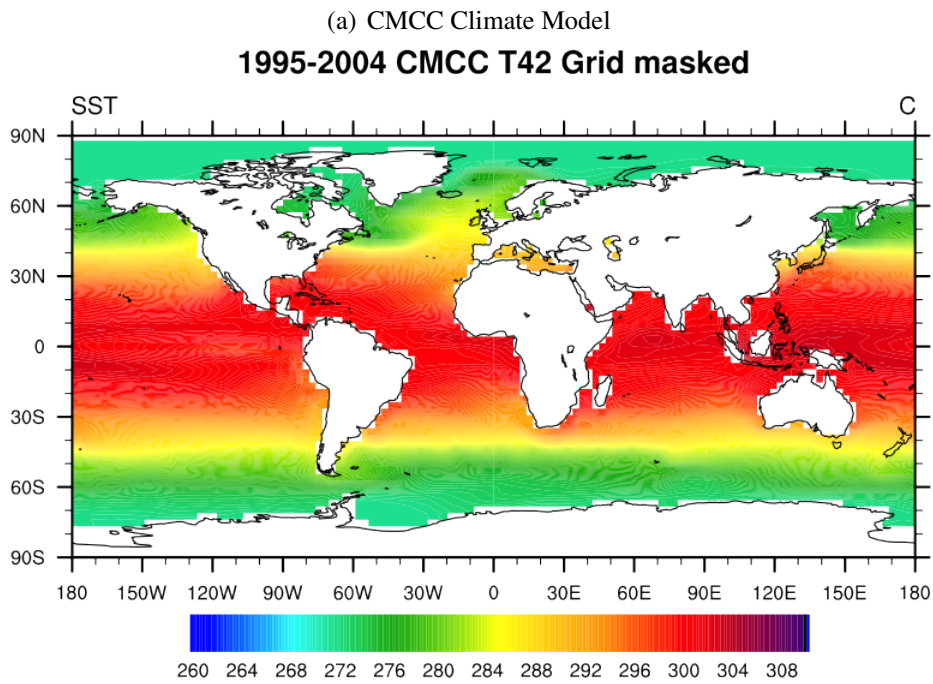


Figure 10: On the top, the global distribution of sea surface temperature in the CMCC climate model is shown. Below, the differences between model and HadISST observations indicate biases in SSTs (Klinger et al., 2014)

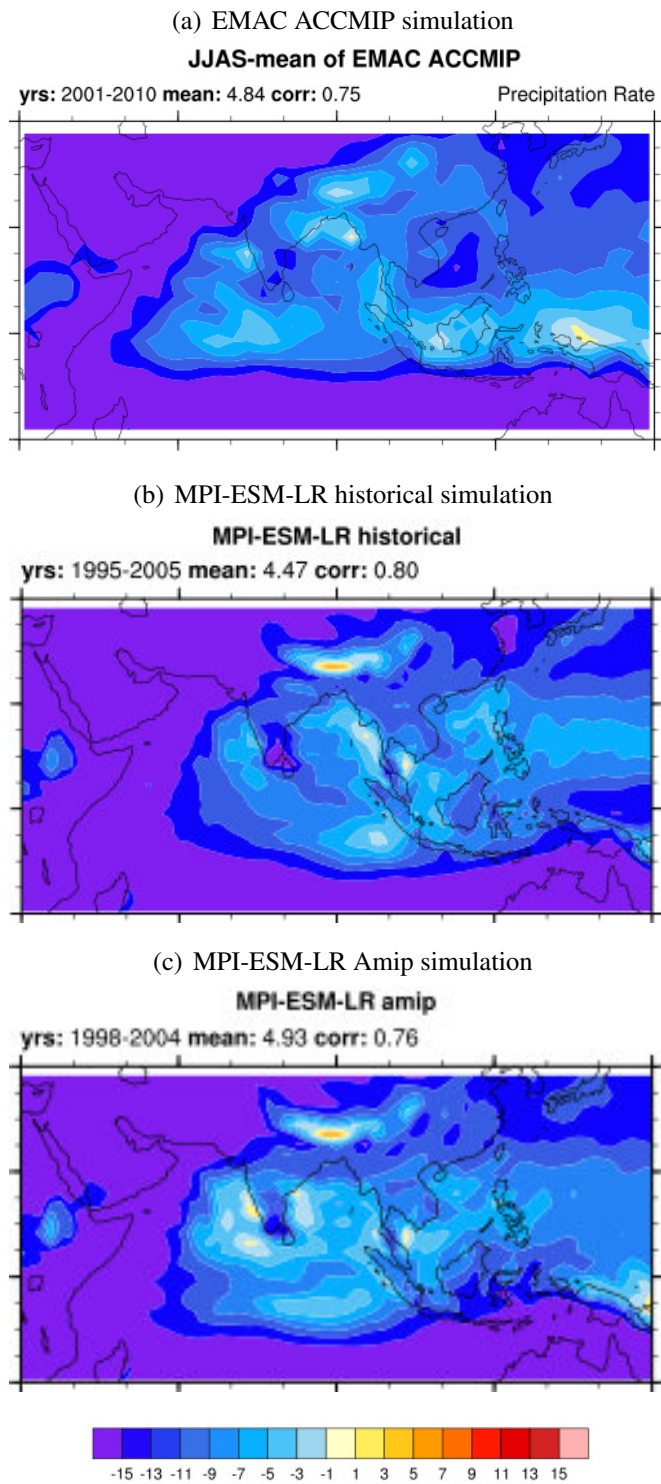


Figure 11: Climatological mean monthly mean precipitation in South Asia for JJAS summer.

This becomes evident when comparing the EMAC ACCMIP simulation to CMIP5 AMIP simulations that also use prescribed SSTs and SICs. In terms of correlation index, the EMAC ACCMIP simulation now performs not worse than the lowest CMIP5 model anymore, but in contrast is in the mid-range of all models used. Compared to the MPI-ESM-LR AMIP simulation (figure 11), which is based on ECHAM6 and hence uses a similar core to EMAC, performance in terms of correlation index is almost identical. Moreover, the MPI-ESM-LR AMIP simulation has a lower correlation index (0.76) than the historical experiment (0.8) and shows more overestimation of precipitation. However, it is important to notice, that the MPI-ESM-LR Amip simulation has been carried out against TRMM observational data while EMAC ACCMIP is originally compared to GPCP-SG data. Thus the EMAC ACCMIP plot showed in figure 11 also uses TRMM as reference model.

5.3.4 Biases in the Simulation of 850 hPa Low-Level Winds

A important feature of the monsoon that is very closely related to precipitation is the circulation especially with its 850 hPa low-level winds. As winds pick up the moisture from the ocean and carry it to the landmass, a misrepresentation either regarding intensity or regarding direction can lead to biases in the simulation of precipitation. According to Sperber et al. (2012), the main features of the low-level monsoon circulation in South Asia include firstly the cross-equatorial flow over the western Indian Ocean and East African highlands followed by the westerly flow extending from the Arabian Sea to the South China Sea. Secondly the monsoon trough over the Bay of Bengal and the weak southerlies over the South China Sea and East Asia are a defining feature of the monsoon circulation.

Figure 12 compares the mean of 850 hPa low-level winds during the monsoon summer season simulated in EMAC ACCMIP to ERA-Interim reanalysis data. It is noticeable that not only for EMAC ACCMIP, but also for CMIP5 models, which are not shown here, the correlation index is significantly higher than for the simulation of precipitation. However, compared to the CMIP5 simulation, the EMAC ACCMIP simulation is performing only slightly better than the worst model of the CMIP5 ensemble with the historical simulations. Although the general features of the circulation are represented quite well, there are clear differences between EMAC ACCMIP and ERA-Interim data (Figure 12).

Comparing the low-level biases to the precipitation biases in the South Asia area leads to the assumption that the biases are related to each other. According to Sperber et al. (2014), a too zonal monsoon trough over the Bay of Bengal may

contribute to excessive rainfall in the vicinity of the South China Sea and the maritime continent. Moreover, underestimation of winds around India and South East Asia are consistent with too weak rainfall over the Gulf of Thailand and the South China Sea.

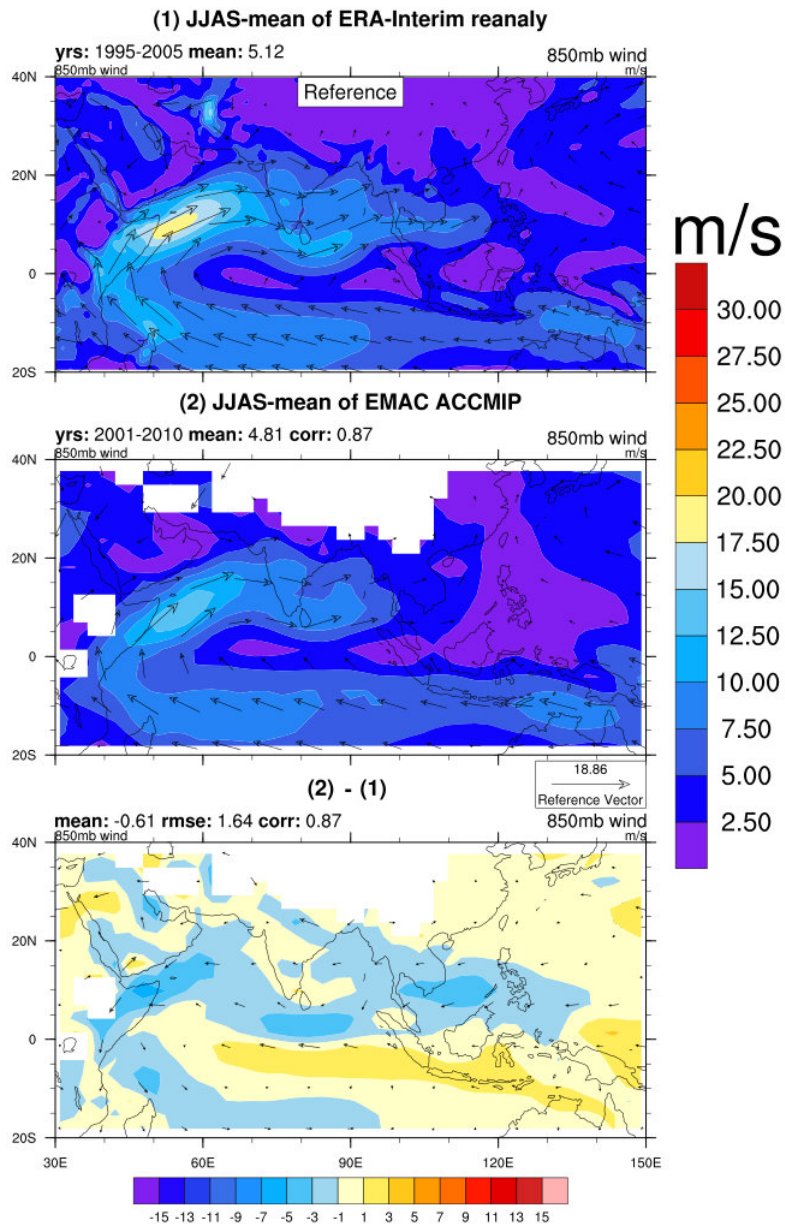


Figure 12: 850 hPa low-level winds for (1) ERA-Interim reanalysis data and (2) EMAC ACCMIP simulation during JJAS summer; Differences between EMAC ACCMIP and ERA-Interim 850hPa low-level winds (bottom).

5.3.5 Biases in Radiation and Cloud Parameterization

As external solar forcing is the main driver of monsoon, biases in radiation can be a possible source of error for precipitation. Also clouds and their parameterization in EMAC can play an important role, given their strong influence on the Earth's radiation budget. When analyzing radiation, two different components have to be considered: incoming solar shortwave radiation, which plays a major role as the monsoon's basic driver, and longwave radiation emitted by the Earth, also contributing to the total radiation budget and influencing the climate.

The sun steadily emits radiation with its peak in the visible and ultra-violet shortwave spectrum. Incoming solar shortwave radiation mainly interacts with low thick marine clouds as well as with mixed layer clouds, that reflect the radiation back to space. The fraction that is reflected back to space is called cloud albedo and turns out to be around 30% of the total incoming solar radiation. Low thick and mixed-layer clouds have a higher reflectance than for example ocean surfaces or rain forests, which leads to more reflection than in the absence of clouds and hence to a cooling effect on the Earth's surface (Chen et al., 2000).

Another important effect to be considered is the infrared longwave radiation emitted by the Earth. It gets absorbed by high thin and mixed-layer clouds, and eventually re-emitted back to Earth or to space. As the top of clouds is colder than the Earth's surface, re-emission back to space is reduced and hence energy is trapped beneath the clouds. Thus the temperature of the Earth's surface as well as the atmosphere increases, an effect called Cloud Greenhouse Forcing.

When evaluating monsoon in climate models, it is important to analyze the representation on clouds and the related uncertainties in order to understand the biases in the representation of precipitations. To that extend, cloud radiative effects (CRE) diagnostics have been developed and implemented in the ESMValTool. The simulated fields of longwave and shortwave radiation, under both clear-sky and all-sky conditions, are compared to the CERES-EBAF satellite data, considering a climatological mean of the 1995-2005 period.

Shortwave cloud radiative effect - MOD-OBS

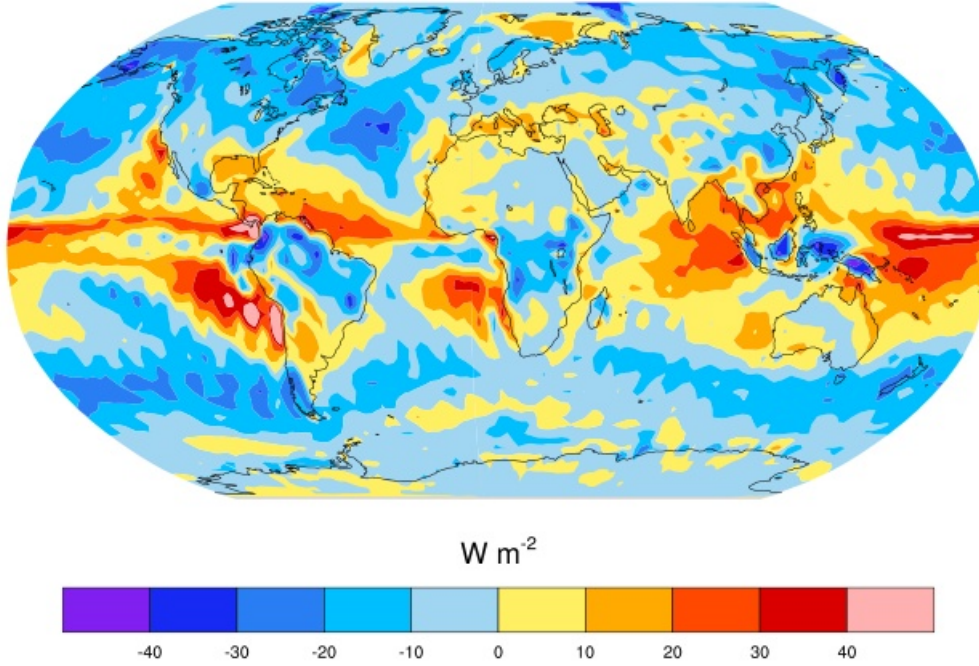


Figure 13: Difference between EMAC ACCMIP and CERES-EBAF satellite data in the global distribution of shortwave cloud radiative effects (clear-sky minus all-sky conditions).

Analogously to figure 9.5. of the Fifth Assessment Report of the Intergovernmental Panel on Climate Change (IPCC) (Flato et al., 2013), the global and zonal-mean distributions of shortwave, longwave and net (shortwave + longwave) cloud radiate effects have been plotted using following definitions:

$$SW_{CRE} = rsutcs - rsut \quad (5.3.1)$$

$$LW_{CRE} = rlutcs - rlut \quad (5.3.2)$$

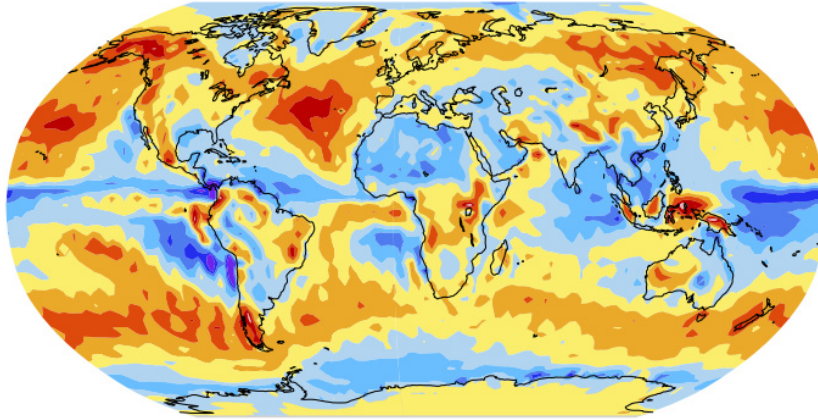
$$NET_{CRE} = SW_{CRE} + LW_{CRE} \quad (5.3.3)$$

Here, rsut and rlut stand for all-sky conditions, while rsutcs and rlutcs represent clear sky conditions.

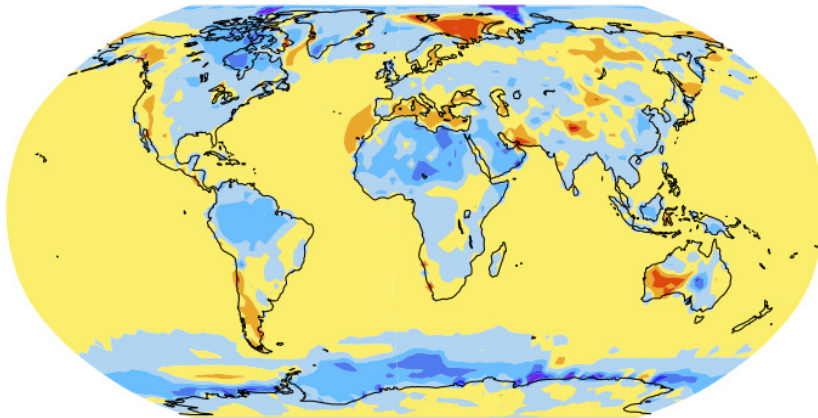
As a first step, the CMIP5 models have been used to exactly reproduce figure 9.5 of IPCC AR5. Then the same diagnostics have been applied to the EMAC ACCMIP simu-

lation. Figure 13 shows the difference between EMAC ACCMIP and CERES-EBAF observations for shortwave cloud radiative effects. Compared to the CMIP5 multi-model mean (not shown here), errors are in general larger.

(a) All-Sky shortwave radiation – MOD-OBS



(b) Clear-Sky shortwave radiation – MOD-OBS



$W m^{-2}$



Figure 14: Analogously to figure 12 but showing all-sky conditions (a) and clear-sky conditions (b) separately for shortwave radiation in EMAC ACCMIP.

To identify which of the radiation variables is responsible for the discrepancy, the same plot has been produced for the clear-sky and all-sky radiation fields, as shown in Figure 14. While clear-sky conditions are simulated very well especially in the South Asian area, all-sky shortwave radiation shows large biases all over the globe. It is noticeable,

that positive biases occur mainly in the mid-latitudes while negative biases occur in the tropics. This points to a possible bias in the representation of low clouds. According to Räisänen and Järvinen (2010), EMAC underestimates the low cloud fraction compared to ISCCP satellite data at low latitudes, but tends to overestimate it at high latitudes (above 45°).

Biases over Alaska and North-East Russia could also be due to snow albedo, which means that the extent of snow is overestimated leading to a higher reflectance than observations indicate. But this quantity has not been evaluated here.

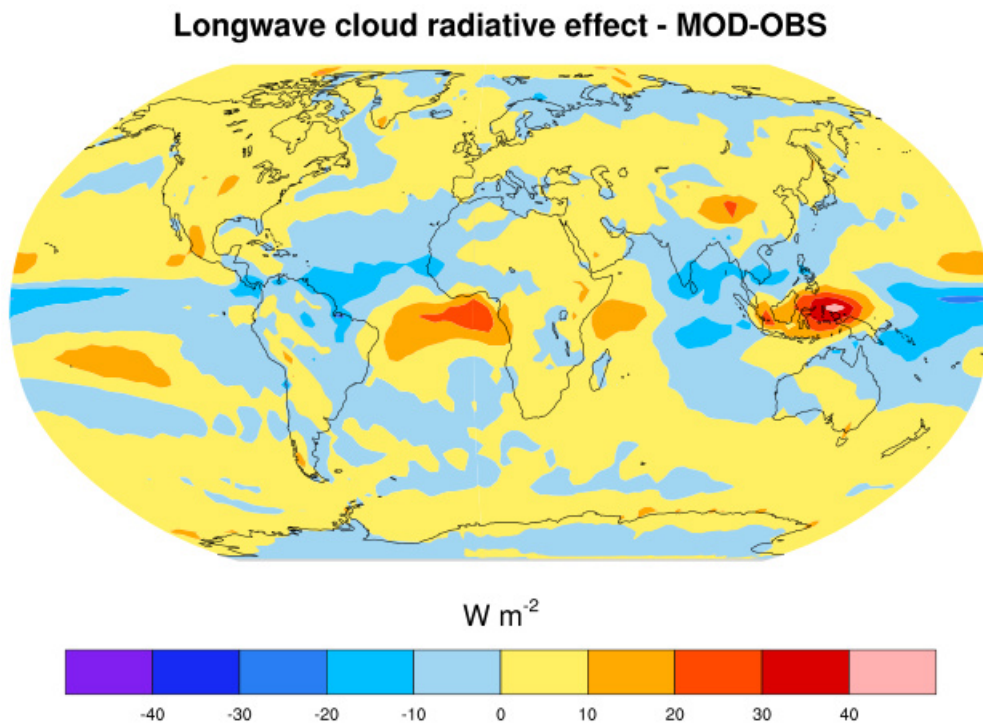


Figure 15: Difference between EMAC ACCMIP and CERES-EBAF satellite data in the global distribution of longwave cloud radiative effects (clear-sky minus all-sky conditions).

Figure 15 shows the longwave cloud radiative effect analogously to the shortwave effect discussed based on figure 13. Here, the bias is clearly smaller than for shortwave radiation with only two major spots of errors located at the Gulf of Guinea and over the maritime continent. The spatial pattern of these biases matches quite well with those of the precipitation during the NDJF winter season in South Asia. As for shortwave radiation, clear sky conditions are simulated very well with only moderate local biases

for the long-wave radiation. However, all sky conditions produce larger deviations than clear-sky conditions (figure 16). Especially over the Indian Ocean south of India, positive biases occur while parts of the maritime continent show a large local negative bias. The strong positive bias in the longwave cloud radiative effect could be due to a higher amount of high clouds in EMAC compared to ISCCP data (Räsänen and Järvinen, 2010).

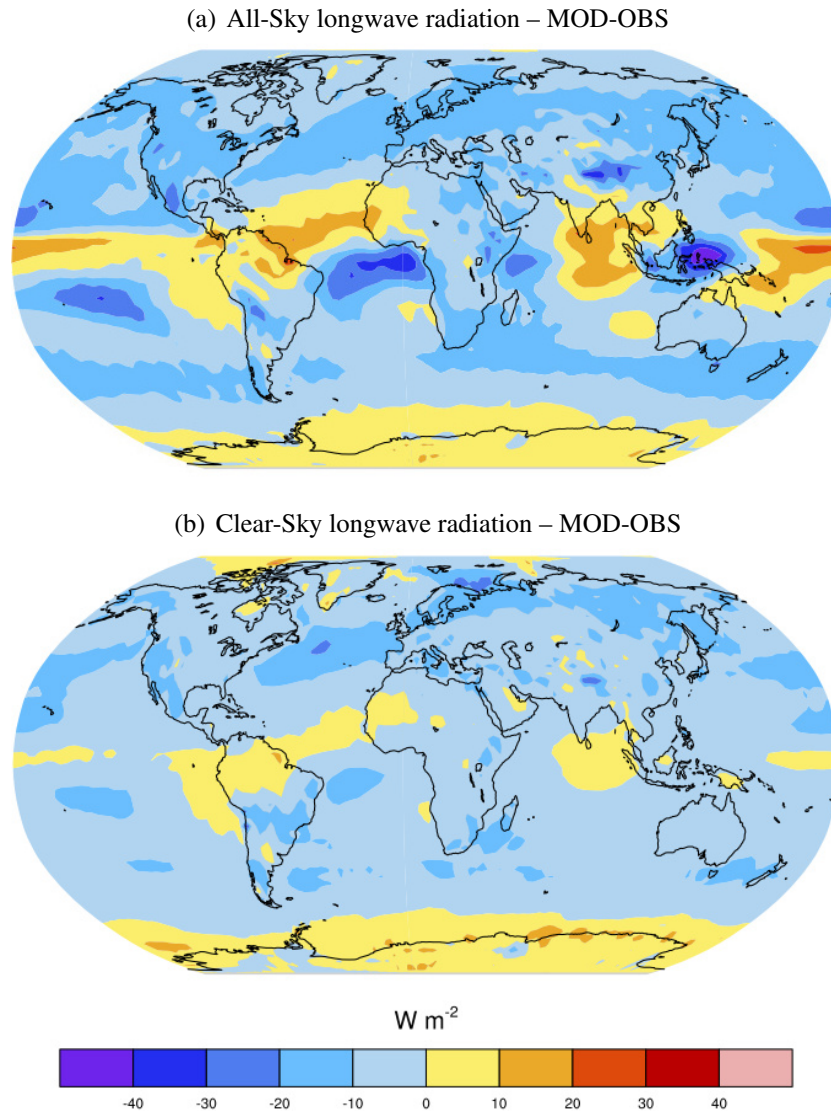


Figure 16: As figure 13, but showing longwave radiation fluxes.

The sum of shortwave and longwave cloud radiative effects yields the net effect of clouds on the Earth's radiation budget. This is shown in figure 16, as the difference between the EMAC ACCMIP simulation and CERES-EBAF observations.

Errors in shortwave- and longwave cloud radiative effects are partly compensating each other in some of the areas but large deviations between simulation and observations are still visible in many regions. In South Asia, both negative and positive errors occur. This gives evidence for a misrepresentation of clouds in EMAC, which could be a possible source of bias in the simulation of monsoon precipitation. However, the climate system is too complex to strictly connect errors in cloud radiative effects to precipitation biases on a local scale. Therefore the above statements are not conclusive and shall be regarded as a possible hint for future investigations.

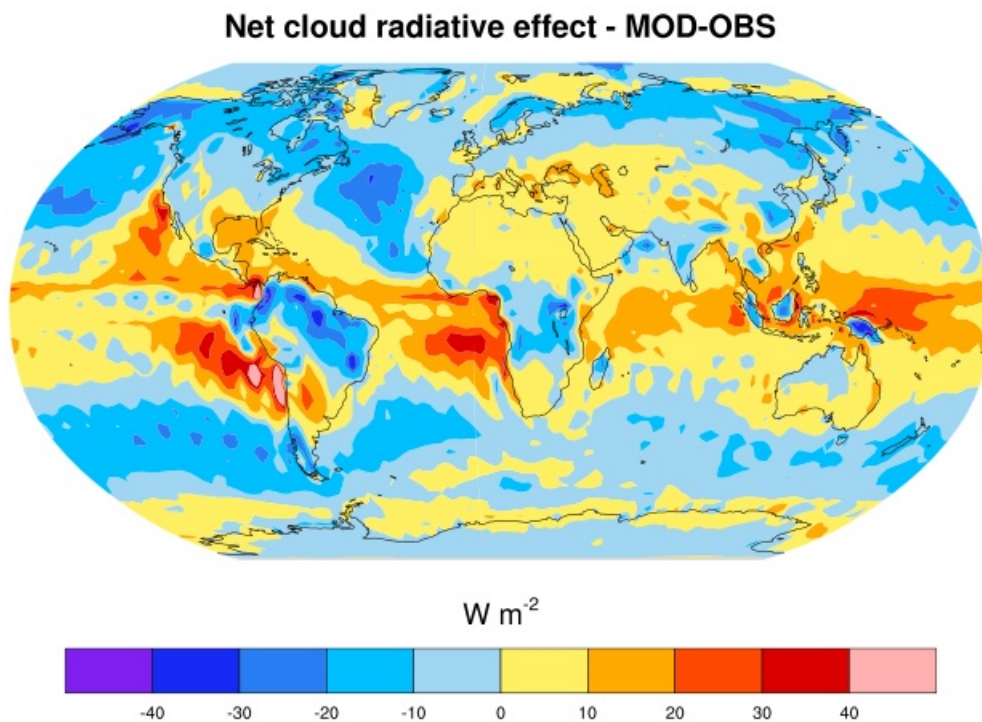


Figure 17: Net cloud radiative effects in EMAC ACCMIP calculated as the sum of shortwave and longwave cloud radiative effects showed before.

5.3.6 Other Influences

Although monsoon is mainly driven by external solar forcing, it also depends on internal feedback processes such as El Niño-Southern Oscillation (ENSO) mainly through changes in the Walker Circulation. According to IPCC AR4 (2007), a strong correlation between ENSO and tropical rainfall and circulation leads in South Asia to less monsoon rainfall in El Niño years and increased rainfall in La Niña years.

As a consequence, biases in the simulation of ENSO and other phenomena are likely to influence the amount of precipitation and resulting monsoon domains as well as the simulated winds. To evaluate the influence of biases in ENSO, further analysis is needed.

6 Summary and Outlook

In this thesis, the South Asian monsoon has been evaluated in the global ECHAM/MESy Atmospheric Chemistry model (EMAC) using the Earth System Model Evaluation Tool (ESMValTool). To place the outcome of this evaluation in a broader context, a comparison to CMIP5 models was also shown. When analyzing the seasonal mean of precipitation in South Asia for both the monsoon summer (June to September) and winter (November to February), EMAC ACCMIP turned out to generally overestimate the amount of precipitation. Moreover, the global monsoon domains (defined as the regions where the mean precipitation difference between summer and winter exceeds 2.5 mm/day) are also overestimated. Considering the correlation between model simulation and observational data as a measure of model's performance, EMAC was found to be worse than the CMIP5 historical experiments considered here in representing precipitation in South East Asia.

To identify the possible reasons for biases, low-level (850 hPa) winds and cloud radiative effects have also been evaluated within the ESMValTool. As for precipitation, EMAC ACCMIP simulates low-level winds worse than models of the CMIP5 historical experiment in terms of correlation index. Detected biases at 850 hPa are likely to have an influence on the representation of rainfall. Furthermore, cloud radiative effects were found to show large biases in South Asia especially for shortwave radiation. As solar shortwave radiation is a major driver for monsoon dynamics, biases in the radiation fields are also likely to contribute to precipitation errors. The reason could be a misrepresentation of low clouds, which are mainly responsible for the reflection of solar radiation (Räisänen and Järvinen, 2010), and high thin clouds over South Asia.

Another possible source for the biases detected in the EMAC simulation is that biases exist in the prescribed sea surface temperatures (SST) and sea ice concentrations (SIC) that are taken from the historical CMIP5 experiment carried out with the CMCC model. Furthermore, the use of prescribed SSTs in general lowers the model performance as errors in SSTs partly compensate errors in precipitation for coupled models (Sperber et al., 2013). Additional work is required to better identify the reasons for the biases in the EMAC simulation found here. In particular, the evaluation could be repeated with an EMAC simulation with prescribed SSTs and SICs from observations and a simulation with a coupled ocean. This would give further insights whether the deviations in precipitation in the EMAC ACCMIP simulation found here are mainly due to the specific boundary conditions used or for example due to the cloud parametrization or the missing coupled ocean.

Finally, differences between the GPCP-SG and TRMM datasets for precipitation suggests that uncertainties exist also in the observational data and that further

improvement of observations is needed in order to better evaluate the performance of climate models.

Further analyses of monsoon in EMAC shall focus on daily high-frequency rainfall data and consider longer time periods, when applying the additional diagnostics available in the ESMValTool. In addition, this study can be used as a basis for further investigations, such as the evaluation of monsoon in the ESMVal HALO Campaign or the CCMI-REF experiments. Finally, the role of monsoon in stratosphere and troposphere exchange can yield additional insights.

7 Acknowledgements

This work was performed as part of the DLR ESMVal (Earth System Model Validation) project and the FP7 project Earth System Model Bias Reduction and assessing Abrupt Climate Change (EMBRACE).

I would like to express my sincere gratitude to my supervisor Veronika Eyring, who has supported me throughout my thesis with her encouragement and effort.

My sincere thanks also go to Mattia Righi and Klaus-Dirk Gottschaldt for all the dedicated support and especially for their help with sorting out NCL problems.

Moreover, I would like to thank Franziska Frank and Daniel Senfleben for always assisting with NCL questions.

Finally, I want to thank the whole DLR-IPA Department 1 for the enjoyable and interesting time.

8 References

- Chen, Ting, William B. Rossow, Yuanchong Zhang, 2000: Radiative effects of cloud-type variations. *J. Climate*, 13, 264–286.
doi: [http://dx.doi.org/10.1175/1520-0442\(2000\)013<0264:REOCTV>2.0.CO;2](http://dx.doi.org/10.1175/1520-0442(2000)013<0264:REOCTV>2.0.CO;2)
- Dee, D. P., Uppala, S. M., Simmons, A. J., Berrisford, P., Poli, P., Kobayashi, S., Andrae, U., Balmaseda, M. A., Balsamo, G., Bauer, P., Bechtold, P., Beljaars, A. C. M., van de Berg, L., Bidlot, J., Bormann, N., Delsol, C., Dragani, R., Fuentes, M., Geer, A. J., Haimberger, L., Healy, S. B., Hersbach, H., Hólm, E. V., Isaksen, I., Kållberg, P., Köhler, M., Matricardi, M., McNally, A. P., Monge-Sanz, B. M., Morcrette, J.-J., Park, The ERA-Interim reanalysis: configuration and performance of the data assimilation system. *Q.J.R. Meteorol. Soc.*, 137: 553–597. doi: 10.1002/qj.828
- Fiore, A.M., Naik, V., Spracklen, D.V., Steiner, A., Unger, N., Prather, M., Bergmann, D., Cameron-Smith, P.J., Cionni, I., Collins, W.J., Dalsoren, S., Eyring, V., Folberth, G.A., Ginoux, P., Horowitz, L.W., Josse, B., Lamarque, J.-F., MacKenzie, I.A., Nagashima, T., O'Connor, F.M., Righi, M., Rumbold, S.T., Shindell, D.T., Skeie, R.B., Sudo, K., Szopa, S., Takemura, T. and Zeng, G., 2012. Global air quality and climate. *Chemical Society Reviews*.
- Flato, G., J. Marotzke, B. Abiodun, P. Braconnot, S.C. Chou, W. Collins, P. Cox, F. Driouech, S. Emori, V. Eyring, C. Forest, P. Gleckler, E. Guilyardi, C. Jakob, V. Kattsov, C. Reason, and M. Rummukainen, 2013: Evaluation of climate models. In *Climate Change 2013: The Physical Science Basis. Contribution of Working Group I to the Fifth Assessment Report of the Intergovernmental Panel on Climate Change*. T.F. Stocker, D. Qin, G.-K. Plattner, M. Tignor, S.K. Allen, J. Doschung, A. Nauels, Y. Xia, V. Bex, and P.M. Midgley, Eds. Cambridge University Press, 741-882.
- Huffman, George J., Robert F. Adler, Philip Arkin, Alfred Chang, Ralph Ferraro, Arnold Gruber, John Janowiak, Alan McNab, Bruno Rudolf, Udo Schneider, 1997: The Global Precipitation Climatology Project (GPCP) Combined Precipitation Dataset. *Bulletin of the American Meteorological Society*: Vol. 78, No. 1, pp. 5-20.
- Huffman, G.J., R.F. Adler, D.T. Bolvin, G. Gu, E.J. Nelkin, K.P. Bowman, Y. Hong, E.F. Stocker, D.B. Wolff, 2007: The TRMM Multi-satellite Precipitation Analysis: Quasi-Global, Multi-Year, Combined-Sensor Precipitation Estimates at Fine Scale. *J. Hydrometeor.*, 8: 38-55.
- IPCC, 2007: *Climate Change 2007: The Physical Science Basis. Contribution of Working Group I to the Fourth Assessment Report of the Intergovernmental Panel on Climate Change* [Solomon, S., D. Qin, M. Manning, Z. Chen, M. Marquis, K.B. Averyt, M. Tignor and H.L. Miller (eds.)]. Cambridge University Press, Cambridge, United Kingdom and New York, NY, USA.
- Jöckel, P., Tost, H., Pozzer, A., Brühl, C., Buchholz, J., Ganzeveld, L., Hoor, P., Kerkweg, A., Lawrence, M., nbsp, G. Sander, R., Steil, B., Stiller, G., Tanarhte, M., Taraborrelli, D., van Aardenne, J. and Lelieveld, J., 2006. The atmospheric chemistry general circulation model ECHAM5/MESy1: consistent simulation of ozone from the surface to the mesosphere. *Atmos. Chem. Phys.*, 6(12): 5067-5104.
- Klinger, C., Eyring, V., Righi, M., Frank, F., Gottschaldt, K.-D., Jöckel, P. and Cionni, I., 2014. Quantitative evaluation of ozone and selected climate parameters in a set of simulations with the ECHAM/MESy Atmospheric Chemistry (EMAC) model. GMD, subm.
- Lamarque, J.F., Shindell, D.T., Josse, B., Young, P.J., Cionni, I., Eyring, V., Bergmann, D., Cameron-Smith, P., Collins, W.J., Doherty, R., Dalsoren, S., Faluvegi, G., Folberth, G., Ghan, S.J., Horowitz, L.W., Lee, Y.H., MacKenzie, I.A., Nagashima, T., Naik, V., Plummer, D., Righi, M., Rumbold, S.T., Schulz, M., Skeie, R.B., Stevenson, D.S., Strode, S., Sudo, K., Szopa, S., Voulgarakis, A. and Zeng, G., 2013. The Atmospheric

- Chemistry and Climate Model Intercomparison Project (ACCMIP): overview and description of models, simulations and climate diagnostics. *Geoscientific Model Development*, 6(1): 179-206.
- Li, J. and Q. Zeng, 2005: A new monsoon index, its interannual variability and relation with monsoon precipitation. *Climatic and Environmental Research*, 10(3): 351-365.
- Loeb, Norman & National Center for Atmospheric Research Staff (Eds). Last modified 26 Mar 2014. "The Climate Data Guide: CERES EBAF: Clouds and Earth's Radiant Energy Systems (CERES) Energy Balanced and Filled (EBAF)." Retrieved from <https://climatedataguide.ucar.edu/climate-data/ceres-ebaf-clouds-and-earths-radiant-energy-systems-ces-eres-energy-balanced-and-filled>
- Naik, V., Voulgarakis, A., Fiore, A.M., Horowitz, L.W., Lamarque, J.F., Lin, M., Prather, M.J., Young, P.J., Bergmann, D., Cameron-Smith, P.J., Cionni, I., Collins, W.J., Dalsoren, S.B., Doherty, R., Eyring, V., Faluvegi, G., Folberth, G.A., Josse, B., Lee, Y.H., MacKenzie, I.A., Nagashima, T., van Noije, T.P.C., Plummer, D.A., Righi, M., Rumbold, S.T., Skeie, R., Shindell, D.T., Stevenson, D.S., Strode, S., Sudo, K., Szopa, S. and Zeng, G., 2013. Preindustrial to present-day changes in tropospheric hydroxyl radical and methane lifetime from the Atmospheric Chemistry and Climate Model Intercomparison Project (ACCMIP). *Atmospheric Chemistry and Physics*, 13(10): 5277-5298.
- Räisänen, P., S. Järvenoja, H. Järvinen, M. Giorgetta, E. Roeckner, K. Jylhä, K. Ruostenoja, 2007: Tests of Monte Carlo Independent Column Approximation in the ECHAM5 Atmospheric GCM. *J. Climate*, 20, 4995-5011.
doi: <http://dx.doi.org/10.1175/JCLI4290.1>
- Roeckner, E., Brokopf, E., Esch, M., Giorgetta, M. A., Hagemann, S., and Kornblueh, L.: Sensitivity of simulated climate to horizontal and vertical resolution in the ECHAM5 atmosphere model, *J. Clim.*, 19, 3771-3791, doi:10.1175/JCLI3824.1, 2006.
- Silva, R.A., West, J.J., Zhang, Y.Q., Anenberg, S.C., Lamarque, J.F., Shindell, D.T., Collins, W.J., Dalsoren, S., Faluvegi, G., Folberth, G., Horowitz, L.W., Nagashima, T., Naik, V., Rumbold, S., Skeie, R., Sudo, K., Takemura, T., Bergmann, D., Cameron-Smith, P., Cionni, I., Doherty, R.M., Eyring, V., Josse, B., MacKenzie, I.A., Plummer, D., Righi, M., Stevenson, D.S., Strode, S., Szopa, S. and Zeng, G., 2013. Global premature mortality due to anthropogenic outdoor air pollution and the contribution of past climate change. *Environmental Research Letters*, 8(3).
- Sperber KR, Annamalai H, Kang IS, Kitoh A, Moise A, Turner A, Wang B, Zhou T (2012) The Asian summer monsoon: an intercomparison of CMIP5 vs. CMIP3 simulations of the late 20th century. *Clim Dyn.* doi:10.1007/s00382-012-1607-6
- Sperber KR, Annamalai H (2014) The use of fractional accumulated precipitation for the evaluation of the annual cycle of monsoons. *Clim Dyn.* doi: 10.1007/s00382-014-2099-3
- Stevenson, D.S., Young, P.J., Naik, V., Lamarque, J.F., Shindell, D.T., Voulgarakis, A., Skeie, R.B., Dalsoren, S.B., Myhre, G., Bernsten, T.K., Folberth, G.A., Rumbold, S.T., Collins, W.J., MacKenzie, I.A., Doherty, R.M., Zeng, G., van Noije, T.P.C., Strunk, A., Bergmann, D., Cameron-Smith, P., Plummer, D.A., Strode, S.A., Horowitz, L., Lee, Y.H., Szopa, S., Sudo, K., Nagashima, T., Josse, B., Cionni, I., Righi, M., Eyring, V., Conley, A., Bowman, K.W., Wild, O. and Archibald, A., 2013. Tropospheric ozone changes, radiative forcing and attribution to emissions in the Atmospheric Chemistry and Climate Model Intercomparison Project (ACCMIP). *Atmospheric Chemistry and Physics*, 13(6): 3063-3085.

- Taylor, K.E., Stouffer, R.J. and Meehl, G.A., 2012. An Overview of Cmp5 and the Experiment Design. *Bulletin of the American Meteorological Society*, 93(4): 485-498.
- Voulgarakis, A., Naik, V., Lamarque, J.F., Shindell, D.T., Young, P.J., Prather, M.J., Wild, O., Field, R.D., Bergmann, D., Cameron-Smith, P., Cionni, I., Collins, W.J., Dalsoren, S.B., Doherty, R.M., Eyring, V., Faluvegi, G., Folberth, G.A., Horowitz, L.W., Josse, B., MacKenzie, I.A., Nagashima, T., Plummer, D.A., Righi, M., Rumbold, S.T., Stevenson, D.S., Strode, S.A., Sudo, K., Szopa, S. and Zeng, G., 2013. Analysis of present day and future OH and methane lifetime in the ACCMIP simulations. *Atmospheric Chemistry and Physics*, 13(5): 2563-2587.
- Wang B, Liu J, Kim HJ, Webster PJ, Yim SY (2012) Recent change of the global monsoon precipitation (1979–2008). *Clim Dyn* 39:1123–1135
- Young, P.J., Archibald, A.T., Bowman, K.W., Lamarque, J.F., Naik, V., Stevenson, D.S., Tilmes, S., Voulgarakis, A., Wild, O., Bergmann, D., Cameron-Smith, P., Cionni, I., Collins, W.J., Dalsøren, S.B., Doherty, R.M., Eyring, V., Faluvegi, G., Horowitz, L.W., Josse, B., Lee, Y.H., MacKenzie, I.A., Nagashima, T., Plummer, D.A., Righi, M., Rumbold, S.T., Skeie, R.B., Shindell, D.T., Strode, S.A., Sudo, K., Szopa, S. and Zeng, G., 2013. Pre-industrial to end 21st century projections of tropospheric ozone from the Atmospheric Chemistry and Climate Model Intercomparison Project (ACCMIP). *Atmospheric Chemistry and Physics*, 13(4): 2063-2090.

Declaration of Authorship

I do solemnly declare that I have written the presented thesis by myself without undue help from a second person others and without using such tools other than that specified. Where I have used thoughts from external sources, directly or indirectly published or unpublished, this is always clearly attributed. Furthermore, I certify that this research thesis or any part of it has not been previously submitted for a degree or any other qualification at the Ludwig-Maximilians-Universitaät of Munich or any other institution in Germany or abroad.

Date,

Signature